Journal of Sustainability Science and Management
Volume 20 Number 2, February 2025: 346-363
eISSN: 2672-7226

OPTIMISING METHYLENE BLUE REMOVAL USING SAGO EFFLUENT ACTIVATED CARBON: A RESPONSE SURFACE METHODOLOGY STUDY

ZAINAB NGAINI*, NUR AQILAH MAKSHUT*, NURUL IWANI MAHMUT, NORAQILAH MOHD ADZMI, NURLIDZA ARSAT AND ABIGAIL VANESSA ZIEM

Faculty of Resource Science and Technology, Universiti Malaysia Sarawak, 94300 Kota Samarahan, Sarawak, Malaysia.

**Corresponding author: nzainab@unimas.my, aqilahmakshut@gmail.com*
http://doi.org/10.46754/jssm.2025.02.011
Received: 29 May 2024 Revised: 15 July 2024 Accepted: 4 August 2024 Published: 15 February 2025

Abstract: Eliminating effluent-containing dyes into the environment urges for eco-friendly and practical solutions. In this work, Sago Effluent Biomass (SEB) and Sago Effluent Activated Carbon (SEAC) were developed as an inexpensive and efficient adsorbent. The SEAC was pyrolysed and chemically activated using sodium hydroxide (NaOH). The characterisation and physicochemical properties of SEB and SEAC were analysed. The efficiency of SEB and SEAC for Methylene Blue (MB) removal was studied at varying initial solution concentrations (2-10 mg/L) and contact times (0-30 minutes). SEAC exhibits a large pore opening (11.17 µm) compared with SEB (0.21 µm). The total surface area was also increased from 8.04 m^2/g (SEB) to 78.863 m^2/g in SEAC. Response surface methodology (RSM) analysis showed SEAC at an initial concentration of 10 mg/L and a contact period of 60 minutes has obtained a maximum removal effectiveness of 92.69% for MB at pH 6. The adsorption of SEB and SEAC both best fit the Langmuir model. SEB had an R^2 value of 0.9919 while SEAC had an R^2 value of 0.9225 and an adsorption capacity of 0.9013 mg/g. Sludge-activated carbon derived from sago effluent is an effective adsorbent for removing MB from aqueous environments. Overall, the high surface area and porous structure make it a sustainable solution for mitigating pollution from sago processing industries.

Keywords: Sustainability, *Metroxylon sagu*, sago waste, sludge, environmental.

Introduction

The textile industry frequently sources dye pollutants in streams. Coloured water that comes from the dying process of plant fibres (cotton) and animal fibres (cotton and silk) is usually released into the environment without proper treatment (Rahimian & Zarinabadi, 2020). Besides textile industries wastewater, other industries such as cosmetics, printing, food, and stationaries are also heavily concentrated with significantly high amount of dyes that contributes to the pollution of the environment (Patil *et al.*, 2020; Somsesta *et al.*, 2020). This dye-bearing wastewater is not degradable due to complex aromatic molecular structures and synthetic organic materials, which contribute to its stability and carcinogenic (Guo *et al.*, 2018).

Around 10,000 different type of commercial dyes are produced and it is estimated that 700,000 tonnes of Methylene Blue (MB) effluent have been released yearly into the aqueous environment (Reza *et al.*, 2020). MB in the water body utilises dissolved oxygen in the water, which causes a high BOD level and disrupts the aquatic ecosystem (Islam, 2020). Thus, it is imperative to remediate MB-containing wastewater before disposing of it in the environment. Typically, wastewater from a larger textile mill is treated before being released into the aqueous environment. Due to the resilience of dyes to light, heat, and various chemicals, even trace amounts may inadvertently enter the environment and persist over time (Mookiah *et al.*, 2020).

Various methods have been reported for eliminating MB from industrial effluent including coagulation, flotation, hyperfiltration, adsorption, and oxidation (Marrakchi *et al.*, 2017; Fazal *et al.*, 2021). Adsorption employing

biomass from agricultural wastes has drawn the most interest among these techniques because of its efficiency, versatility, low treatment costs, and ease of design (Devanna *et al*., 2019). Many studies highlighted the remarkable efficacy of various types of biomasses in adsorbing MB from wastewater. Notable examples include the fruit shell of the *wodyetia bifurcate* (dos Santos *et al.*, 2019), algae from the *porphyridium* sp. (Buhani *et al*., 2019), and *spirulina* sp. microalgae (Kausar *et al.*, 2020).

However, modifying biomass through chemical and physical activations can further help improve pore structures and surface area, making it more reliable for adsorption. Activated Carbon (AC) is particularly noted for its excellent adsorption capacity due to its large surface area, pore volume, and porosity (Devanna *et al.*, 2019). Typically, precursors from inexpensive, otherwise unusable agricultural waste and by-products are utilised to prepare AC. Many studies reported on higher adsorption capacity of MB using AC such as almond bark AC (Rahimian & Zarinabadi, 2020), corn cob AC (Aljeboree *et al.*, 2019), and water hyacinth AC (Nibret *et al.*, 2019). The conversion of agricultural wastes into AC enhances the adsorption performance and mitigates environmental problems and pollution associated with agriculture (Islam *et al.*, 2017).

Sago industries in Sarawak, Malaysia, generate substantial agricultural waste during starch production, presenting a potentially low-cost alternative material for use as adsorbents to remove MB. Previously, sago wastes AC such as bark was esterified and reported to have good adsorption for engine oil removal (7.5 g/g) (Ngaini, 2017). Besides adsorption, sago bark was also employed to produce esterified oil for engines (Wahi *et al.*, 2019). Sago *hampas* were studied to have excellent adsorption on MB with an adsorption capacity of 7.69 mg/g (Rajan *et al.*, 2018). However, based on recent precedent, research has yet to be done on using sago effluent as a solid adsorbent to remove pollutants such as dyes. Sago effluent is often used as cultivation media for spirulina (Phang *et al.*, 2000) and syngas (Mariathankam *et al.*, 2020; Sheela & Asha, 2020). The employment of agricultural wastes as adsorbents of pollutants is well-known among researchers due to their effectiveness, low cost, and practical handling.

Herein, we report the synthesis of AC from sago effluent via sludge formation. The effectiveness of the sludge AC for MB removal was studied in batch adsorption experiments. The results demonstrate that this method is highly effective, offering a sustainable solution for dye contaminant removal in wastewater treatment.

Materials and Methods

Synthesis of Untreated Adsorbent

Sago Effluent (SE) was collected from Henderson Sago Industries, Sarawak. For the aerobic treatment, SE (20 L) was aerated in a tank for seven days using an Activated Sludge Procedure (ASP) to produce biomass (SEB). The SEB was sieved using a 45 µm sieve and then pyrolysed in a 1,200 Mini Tube Furnace T1-01200-50SL with N^2 gas for 30 minutes at 400°C. The resulting char was immersed in 5 M NaOH (Li *et al.*, 2018), filtered, washed to pH 7, and oven-dried (100°C-105°C). After 24 hours, the char was introduced to a second pyrolysis at 500°C for 90 minutes. HCl (5M, 5 mL) was added to the char product to eliminate the impregnating salt and washed to a pH of 4 using distilled water (Wahi & Senghie, 2014). The solid was oven-dried (105°C, 1 hour) to form SEAC (2.8 g).

Physicochemical Characteristics of Adsorbent Proximate Analysis

The moisture, ash, volatile matter, and fixed carbon content of SEB and SEAC were ascertained using a methodology modified from ASTM D-3173-D-3175. The samples were treated using the method reported (Wahi & Senghie, 2014). The proximate analysis was calculated using the following procedures (Rajan *et al.*, 2018).

Instrumental Analysis

SEB and SEAC were characterised using a JEOL JSM-6390LA scanning electron microscope (SEM) for their surface morphology. The SEB and SEAC samples were thinly coated with platinum film using an Auto Fine Coater (JEOL JFC-1600). The electronic signals were gathered, examined, and converted into pixels on the display to create a surface topography image of the sample. The surface area was analysed using Brunauer-Emmett-Teller (BET) (Quantachrome ASIQC0000-3). The functional groups in SEB and SEAC were characterised by Fourier Transform Infrared (FTIR) analysis using an IS10 Thermo Scientific Nicolet in KBr powder. A UV-visible spectrophotometer (Jasco V-630) was used to measure the MB concentration during batch adsorption analysis.

Batch Adsorption Analysis of MB

Batch adsorption analysis of MB was examined at 2, 4, 6, 8, and 10 mg/L with the solution's initial concentration. The pH 7 of the solution, MB solution (50 mL), adsorbent dosage (0.5 g/50 mL), contact time (30 minutes), and mixing speed (260 rpm) were maintained. A certain amount of solution was put into a quartz cuvette and the wavelength was examined between 500 nm and 700 nm. The final concentration of MB after adsorption was calculated using a calibration graph of the standard solution as a guide. The calculation of removal efficiency was calculated as follows (Rajan *et al.*, 2018). The impact of contact time on MB adsorption was evaluated at intervals of 5, 10, 15, 20, 25, and 30 minutes while the parameters of MB solution volume (50 mL), solution pH of 7, adsorbent dosage (0.5 g/50 mL), MB concentration (10 mg/L), and mixing speed (260 rpm) maintaining constant.

Isotherm Study of MB

The adsorption of MB on SEAC was ascertained using the surface morphology adsorption isotherm. Two type of models were analysed: The Freundlich and Langmuir isotherms. The Langmuir isotherm was performed following the reported method (Doke & Khan, 2017; Rajan *et al*., 2018; Somsesta *et al*., 2020). Meanwhile, the Freundlich isotherm was calculated as follows (Miyah *et al*., 2018).

RSM Analysis

RSM technique that uses qualitative data from pertinent studies to determine how each variable influences experiment results was used by relating how each variable interacts with the others (Makshut *et al*., 2020). Central Composite Design (CCD) was used to identify the independent variables for maximum MB adsorption with the minimum number of experimental runs (Gholamiyan *et al*., 2020). The initial concentration of the solution (0–10 mg/L), pH (2–10), and contact duration (0–30 min) were the operating factors selected for the adsorption of MB on SEAC. The trial version of Design Expert 7.6.1 produced 20 experimental standards.

Results and Discussion

Physicochemical Characteristics of Adsorbent

Proximate Analysis

The ASP procedure produced 94 g of SEB from 20 L effluent. The physicochemical data of untreated Sago Effluent Biomass (SEB) and Sago Effluent Activated Carbon (SEAC) is shown in Supplementary file: Table 1S. The moisture content of SEB was decreased from 0.51% to 0.00% in SEAC. Additionally, the volatile matter decreased from 0.084% to 0.00% following the high-temperature carbonisation and activation. The relatively low moisture and volatile matter content were due to the dried samples used during the analysis. Samples were kept dry in a desiccator to prevent extra moisture from the air trapped in the samples.

The low moisture content of SEB is a good characteristic of an excellent precursor for AC production. The precursor with more than 30% moisture content needs more heat to remove moisture during pyrolysis instead of producing

biochar. In this manner, the high moisture content in a precursor decreased biochar yield (Jankovi *et al.*, 2019). The elevated carbonisation temperature facilitates the breakdown of weaker bridges and bonds within the organic matrices of the samples, releasing a significant amount of volatile matter (Pedicini *et al.*, 2020).

Compared to other biomass waste, the ash content found in SEB is considerably high (99.10%). After activations, the ash content increased slightly to 99.90% in SEAC, indicating the amount of non-volatile inorganic residue and minerals such as Ca, Mg, and K in the sample (Akila *et al*., 2019). The minerals in SE are higher compared with other wastes (P: 0.12 mg/L, K: 50.71 mg/L, Mg: 7.94 mg/L, Ca: 2.62 mg/L), which makes it suitable for bioethanol and biogas production (Hammado *et al*., 2018). High ash content in SEB promotes char formation since the organic elements in the ash are known to catalyse char formation during pyrolysis (Pedicini *et al.*, 2020). Besides minerals and non-volatile matter, the ash content is highly dependent on the building materials such as the composition of lignocellulosic and starch materials in the sample (Siruru *et al.*, 2020). When compared with other sago wastes, SEB has the highest ash content, followed by dregs (3.65%), and bark (0.4%) (Rambli *et al.*, 2019). This is related to the high lignin and cellulose content in sago dregs (Lignin: 7.5%, cellulose: 26.0%) and bark (Lignin: 29.4%, cellulose: 44.0%). Lignin is the material that gives a sturdy structure to bark and dregs while cellulose is the lignin structure's support system (Husin *et al.*, 2019). Both sago dregs and sago bark wastes also contain low starch (49.5% and 22.3%, respectively) while SEB contains 65.70% sago starch (Husin *et al.*, 2019; Siruru *et al.*, 2020).

The slight increment in ash content after pyrolysis and activations was due to the high pyrolysis temperature and NaOH concentration (Lam *et al.*, 2017; Su *et al.*, 2020). Although adsorbents with high ash content might affect the adsorption by forming by-products from the undesired catalytic reaction, the adsorption of MB using SEB and SEAC is unexpectedly high (90.7% and 98.19%, respectively). The high amount of ash in SEB resulted in a low fixed carbon content of 0.22% and decreased to 0.080% in SEAC.

Surface Methodology Analysis

The adsorbents' BET surface area was successfully improved by pyrolysis and chemical activation, rising from 8.04 m^2/g (SEB) to 76.86 m^2/g (SEAC). The surface area of an adsorbent is commonly dependent on the carbonisation temperature. More surface area is usually produced at higher temperatures (Kumar *et al.*, 2018). The adsorbent underwent chemical activation with NaOH. Pore enlargement associated with NaOH was caused by redox reduction and oxidative modification (Islam *et al*., 2017). The pore openings were widened due to the alkaline and carbonate metal that intercalated with the carbon matrices upon chemical activation with NaOH (Islam *et al*., 2017; Rajan *et al*., 2018). The second pyrolysis was conducted at 500°C (90 minutes) at a higher temperature and the pore size was successfully broadened with new pores forming in the current pore walls (Rafiq *et al.*, 2016). A study on apple tree branches also showed that biochar pyrolysed at a higher temperature showed a broadened pore structure, higher surface area, and thermally stable with increasing total carbon (Supriya *et al*., 2019).

Figure 1 shows the surface morphology of SEB and SEAC. The average pore size for SEB [Figure 1 (a)] was 0.71-1.21 µm and increased to 11.17 µm in SEAC [Figure 1 (b)]. The significant increase in the pore size of SEAC was due to the carbonisation process that occurred during the first pyrolysis associated with the removal of volatile matter (González-García, 2018). Irregular surface areas were also observed with large pores that resulted from the treatment with NaOH and pyrolysis at 500°C, which weakens the precursor pore structure and creates larger pores (Wahi *et al.*, 2009). A large NaOH: Char ratio caused pores to merge into each other and collapse to produce larger pores (Khanday

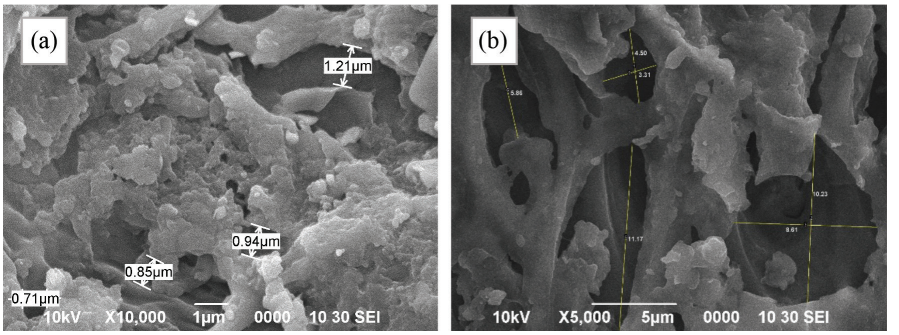

Figure 1: The SEM micrograph of (a) SEB and (b) SEAC

et al., 2017). Moreover, the formation of tars that might clog the pores of the adsorbent was avoided when NaOH was used during activation (Sharma *et al.*, 2015).

The total surface area of SEAC increased significantly due to the formation of pores and collapsing walls. In this study, the total surface area of SEB remarkably increased from 8.04 m²/g to 76.86 m²/g. Higher carbonisation temperatures result in a larger surface area and greater thermal stability (Kumar *et al.*, 2018). Large pore sizes were produced by double physical activation (pyrolysis) and chemical treatment with NaOH increased the total surface area (Rajan *et al.*, 2018).

Functional Group Characterisation

The FTIR spectra of SEB and SEAC are depicted in Figure 2. The broad peak of SEB corresponding to υO-H at 3,408 cm^{-1} was reduced and shifted to 3,421 cm^{-1} after the double carbonisation and activation process in SEAC. The carbonisation process induced high temperatures and chemical treatment that dehydrated the samples, released volatile materials and caused the functional groups to break down after pyrolysis (Rafiq *et al.*, 2016). The shifting of the peak is also the result of chemical activation with NaOH that caused a slight change in the environment of the hydroxyl group. Carboxylic acids in SEB were deprotonated, forming carboxylate anions

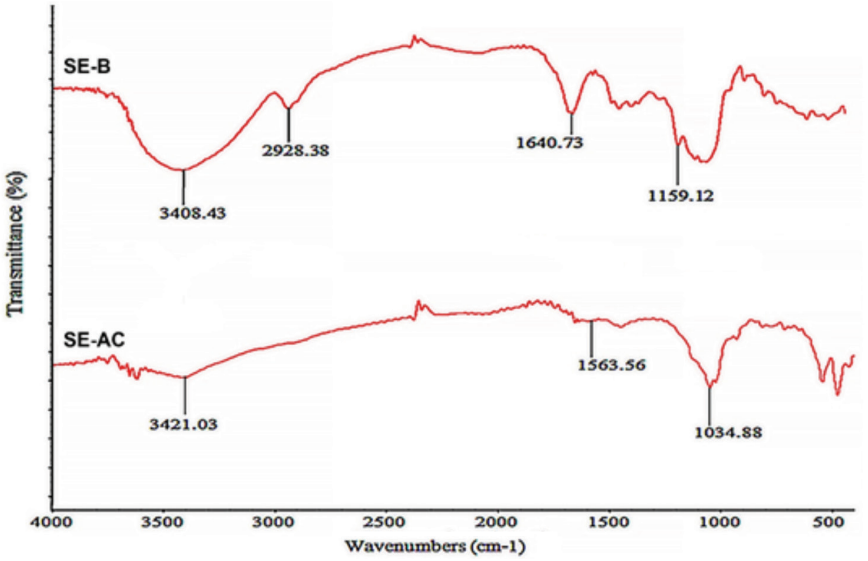

Figure 2: IR spectra of SEB and SEAC

(R-COO-), which makes the OH bond stretching weaker at 3,421 cm^{-1} (Teğin *et al.*, 2024). The v_{C-H} stretching (-CH_2, -CH_3) at 2,928 cm^{-1} was present in SEB and disappeared in SEAC as the result of the vibration of cellulose in the activated carbon (Hedge *et al.*, 2015). The presence of v_{C-O} and $v_{C=C}$ at 1,540 cm^{-1} is attributed to hemicellulose and lignin. The peak was also reduced in SEAC as the lignocellulosic materials were exposed to high pyrolysis temperatures (Kumar *et al.*, 2018). The activation with NaOH led to observing peaks corresponding to C-N, N-H, and N-O stretching in SEAC within the range of 1,034.88-1,563.56 cm^{-1} (Mary *et al.*, 2016).

The -OH groups present in SEAC bind with the dimethylamino group and nitrogen atom in the MB (Dahlan *et al.*, 2019). The IR spectrum of SEAC is similar to most AC derived from other precursors. The washing of SEAC with distilled water after chemical activations followed by the second pyrolysis has removed most chemicals bonded with SEAC, leaving small holes (porosity) for binding with MB. The adsorption of MB onto SEAC is agreeable with the isotherm study conducted; thus, surface functional groups do not always take part in the adsorption process (Patil *et al.*, 2020).

Batch Adsorption Study

The efficacy of MB removal by SEB and SEAC is demonstrated in Figure 3 (a) at varied initial solution concentrations, fixed pH 7, 0.5 g/50 mL adsorbent dosage, and 30-minutes contact period. Both MB removal efficiencies showed the same trend with decreasing removal as the MB solution's initial concentration increased from 0 to 10 mg/L. The highest adsorption occurred when the initial concentration was 2 mg/L with SEAC as adsorbent (99.99%). Slight fluctuation occurred at 8 mg/L of adsorption with SEB and SEAC (71.79% and 98.18%, respectively). The initial concentration of a solution is a significant element in promoting the driving force of a molecule and improving the mass transfer resistance of different phases (Li *et al.*, 2020). As the concentration increases, the removal efficiency decreases. This phenomenon is due to fewer binding sites being available at greater concentrations, which limits the mass transfer of MB molecules (Ebrahimi & Kumar, 2021). The fluctuation occurred at 8 mg/L in both adsorptions with SEB and SEAC, suggesting that more spontaneous effective collisions occurred during the agitation (Baalamurugan *et al.*, 2020). This adsorption trend also supported the monolayer adsorption of MB onto the surface of SEB and SEAC (Somsesta *et al.*, 2020).

The effect of contact time for the MB removal using SEB and SEAC at a fixed pH of 7 at the initial concentration of 10 mg/L and the adsorbent dosage of 0.5g/50 mL is depicted in Figure 3 (b). The removal of MB increased dramatically from 0-30 min. Both adsorptions with SEB and SEAC show the same trend. The highest removal occurred at 30 minutes contact time, 90.70% and 98.55% for SEB and SEAC, respectively. A longer contact time is required to reach equilibrium because of the diffusion process between the adsorbent and adsorbate (Marrakchi *et al.*, 2017). A shorter contact time reduces the opportunity for an effective collision between MB molecules and adsorbents, causing low removal efficiency. The adsorption process with SEB and SEAC is fast and effective, requiring only 30 minutes to reach equilibrium. This rapid adsorption suggests a strong electrostatic interaction between the negatively charged adsorbent surface and the molecule in MB (Ao *et al.*, 2018).

The findings of both trials show that the adsorption with SEAC is substantially greater than the adsorption with SEB. In addition to reaction parameters, including concentration, pH, contact time, and mixing rate, the adsorbent's surface morphology is a significant factor in determining the removal effectiveness. The higher removal of MB by SEAC is due to the enlargement of pores and the creation of new pores following activation with NaOH. This process results in a significantly larger total surface area for SEAC (76.86 m^2/g) than SEB (8.04 m^2/g). The significant improvement in surface area and pore structure after activation provides more binding sites for MB (Jankovi *et al.*, 2019).

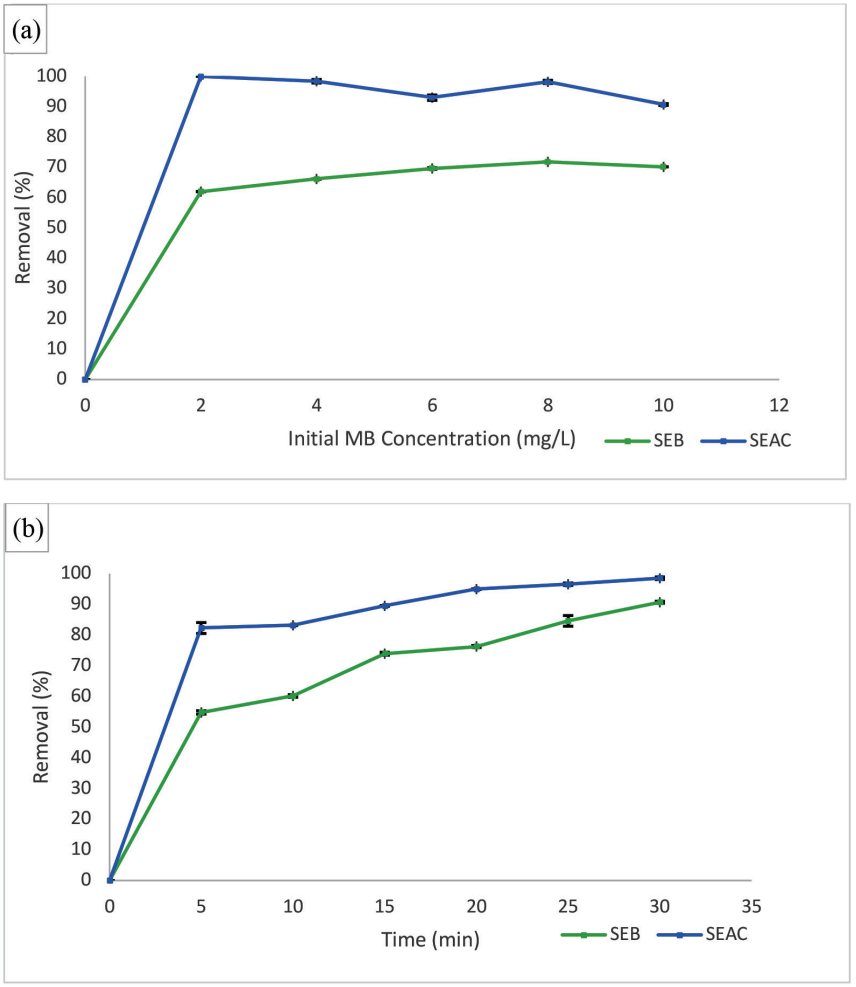

Figure 3: The effect of (a) initial concentration on MB adsorption by SEB and SEAC and (b) contact time on MB adsorption by SEB and SEAC

Adsorption Isotherm

The adsorption isotherm study (Freundlich and Langmuir isotherm) was conducted by manipulating the initial MB concentration (2-10 mg/L), pH 7, adsorbent dosage (0.5 g/50 mL), mixing speed (260 rpm), and contact time (30 minutes) using both SEB and SEAC. Figure 4 shows the Langmuir and Freundlich linear regression model plot. It can be observed via comparison of correlation coefficient values (R^2) that the adsorption isotherm for MB removal using SEB is best fitted with the Freundlich isotherm and the MB removal using SEAC is best described using Langmuir isotherm.

Based on Figure 4 (a), the R^2 for SEB in Langmuir isotherm was 0.7438, which is lower than the Freundlich R^2 value of 0.9915 [Figure 4 (b)]. The 1/n values were -1.3129 and the K_f value was 0.5516. These phenomena implied that the removal of MB with SEB is multilayer adsorption on a heterogeneous surface with various energy distributions (when $1/n < 1$) (Araujo *et al.*, 2021). The n values of a Freundlich isotherm indicate the degree of non-linearity between the concentration of the solution and adsorption. Based on the plotted graph of adsorption with SEB, the n value was

-0.762, a negative value which indicated that the adsorption is irreversible and a chemical process is involved (Makshut *et al.*, 2020).

In Figure 4 (a), the R^2 value for MB removal using SEAC in the Langmuir isotherm was 0.9225, which was higher than the R^2 value in the Freundlich isotherm model (0.8527), as shown in Figure 4 (b). The best fit to the Langmuir isotherm suggests that the adsorption process involves monolayer adsorption onto the homogeneous adsorbent surface, with no interactions occurring between adjacent sites or MB molecules (Nibret *et al*., 2019). The constant b obtained from the Langmuir linear graph was 13.940 L/mg, showing high adsorption energy and contributing to the fast increment in adsorption and various MB concentrations (Miyah *et al*., 2018).

Comparing SEAC to the other ACs shown in Table 1, the maximum adsorption capacity of 0.9012 mg/g was a rather high value. Most studies conducted the adsorption at a longer contact time (1-3 h) and slightly acidic pH compared to the present study. The longer contact time conducted by other studies elongated the adsorbate exposure with the adsorbent's surface, thus, increasing the chance of effective collision (Araujo *et al.*, 2021). Nevertheless, in batch adsorption, there is a high removal of MB (98.55%) despite the low Q_{max} value.

The separation factor (R_L) for the removal of MB with SEAC was 0.034, indicating that the adsorption onto SEAC is favourable ($0 < R_L < 1$). Calculated parameters for Langmuir and Freundlich isotherm for adsorbents and correlation coefficient value, R2 obtained by the linear fitting method are listed in the Supplementary file: Table 2S. The effectiveness of SEB and SEAC in removing MB is shown in Figure 3 (a) at fixed pH 7, 0.5 g/50 mL adsorbent dosage, 30 minutes contact duration, and different initial concentrations. Both MB removal efficiencies displayed the same pattern, with removal declining as the initial MB solution concentration rose from 0 to 10 mg/L. The maximum adsorption was achieved with SEAC as the adsorbent (99.99%) at an initial 2 mg/L concentration.

Table 1: Maximum adsorption capacity (Qmax) for MB removal by various adsorbents using Langmuir isotherm model

	Adsorbent	Q_0 mg/g	Adsorption Condition	Authors
(i)	Palm oil residue AC	48.84	MB concentration: 750 mg/L Adsorption time: 3 h Adsorbent dosage: 0.2 g/100 mL Mixing rate: 120 rpm pH: 7	(Araujo *et al.*, 2021)
(ii)	Eucalyptus residue AC	977.00	MB concentration: 220 mg/L Adsorption time: 24 h Adsorbent dosage: 0.01 g/100 mL Mixing rate: 150 rpm pH: 7	(Han *et al*., 2020)
(iii)	Corn cob AC	216.60	MB concentration: 100 mg/L Adsorption time: 50 min Adsorbent dosage: 0.12 g/100 mL Mixing rate: 110 rpm pH: 5.6	(Jawad *et al*., 2018)

(iv)	Pumpkin peels AC	198.15	MB concentration: 200 mg/L Adsorption time: 3 h Adsorbent dosage: 0.5g/100mL Mixing rate: 110 rpm pH: 7	(Rashid *et al.*, 2019)
(v)	*Citrus lanatus* rind AC	231.48	MB concentration: 100 - 400 mg/L Adsorption time: 2 h Adsorbent dosage: 0.0016g/mL Mixing rate: 130 rpm pH: 5.45	(Üner & Bayrak, 2018)
(vi)	Sago effluent AC	6.85	MB concentration: 10 mg/L Adsorption time: 30 min Adsorbent dosage: 0.1g/100mL Mixing rate: 260 rpm pH: 6	Present study

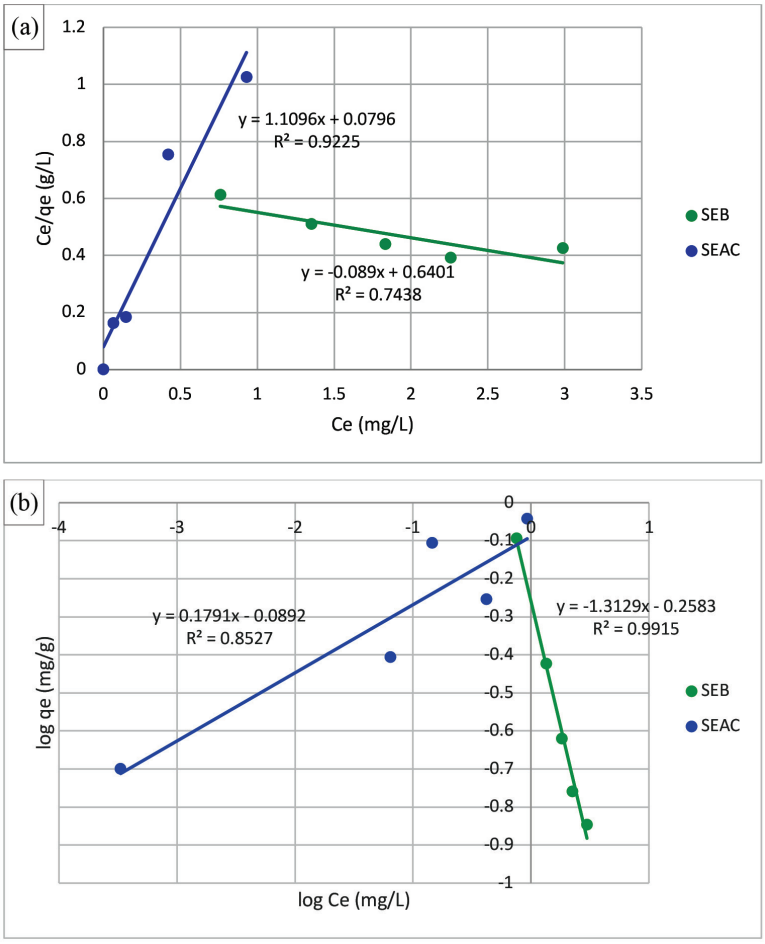

Figure 4: (a) Langmuir isotherm plot for MB adsorption by SEB and SEAC and (b) Freundlich isotherm plot for MB adsorption by SEB and SEAC

RSM Study

The RSM study was conducted on removing MB using SEAC as an adsorbent. Based on the batch adsorption study, the adsorption employing SEAC yields more promising results and high adsorption efficiency. Thus, SEAC is more favourable to use as an adsorbent than SEB. The ranges and responses of 20 experimental runs are shown in the Supplementary file: Table 3S). SAC removed between 58.15% and 92.69% of the MB. The experimental settings of pH (10), initial MB concentration (2 mg/L), and contact time (30 minutes) resulted in the lowest MB elimination (58.15%) as in Run 2. The highest removal was 92.69%, which occurred under the following conditions: pH (6), initial concentration (10 mg/L), and contact time (60 minutes).

The highest-order polynomial based on a quadratic model of Design Expert Software served as the basis for this recommendation (Chaduka *et al.*, 2020). The model was selected when the additional terms were significant. Equation 1 is the final empirical model expressed in terms of coded components.

$$\text{Percentage adsorption of MB} = +87.98 - 2.98A + 12.51B + 1.55C + 1.74AB + 0.730AC - 0.6938BC - 0.0155A^2 - 8.75B^2 - 0.3751C^2 \quad (1)$$

The effects of the variables on the responses of the percentage removal of MB are represented by the coefficients with one variable, pH (A), initial concentration (B), and contact duration (C). A quadratic effect and the correlation between the variables are displayed by the coefficient with two distinct variables (Priyanka *et al.*, 2019; Makshut *et al.*, 2020). A positive symbol indicates a synergistic impact while the antagonistic effect is shown by a negative symbol (Chaduka *et al.*, 2020).

The experimental data (Figure 5) fitted the constructed model quite well, as indicated by a high R^2 value of 0.999 (Kumar *et al*., 2020). There is a decent agreement between the adjusted R^2 (0.998) and the projected R^2 (0.997). The signal-to-noise ratio is measured by an Adeq precision, ideally higher than 4. The model is sufficient and useful for navigating the design space, as indicated by the ratio of 113.0483 (Makshut *et al*., 2020). The Coefficient of Variance (CV) value is a percentage that represents the ratio of the observed response's mean value to the standard error of estimations. The model's reproducibility is demonstrated by the CV value of 0.485%, which was less than 10% (Gholamiyan *et al.*, 2020; Kumar *et al.*, 2020).

Figure 5 illustrates the percentage removal of MB based on the RSM study. The combined effects of contact time and initial concentration are displayed in Figure 5 (a) with the following experimental parameters fixed: Adsorbent dosage 0.5 g/50 mL, mixing rate 260 rpm. At an initial concentration of 10 mg/L and pH 10, more elimination was observed at 90 minutes of contact time (91.45%) compared to 60 minutes (88.11%). MB molecules will diffuse into the porous structure at the adsorbent surface after penetrating the boundary layer. This procedure will take a fair amount of time, as longer contact time increases the mass transfer driving force, thereby enhancing the adsorption of MB (Amode *et al*., 2016; Jawad *et al.*, 2016; Hu & Gholizadeh, 2019).

The removal of MB was lower (69.30%) when the initial concentration was 2 mg/L but higher removal of MB (92.17%) when the initial concentration was 10 mg/L at 30 minutes contact time and pH 2. The contact time (30 minutes) is observed to be too long for removing a lower concentration of MB. This is due to the detachment of MB from the SEAC surface during a long agitation time (Nasrullah *et al.*, 2018). Desorption occurs after the adsorption reaches equilibrium at a certain time (Araujo *et al.*, 2021).

Figures 5 (b) and (c) display the combined effects of initial concentration (pH) and contact time (pH). At the initial concentration of 10 mg/L and the contact time of 60 minutes, a higher clearance occurred at pH 6 (92.69%).

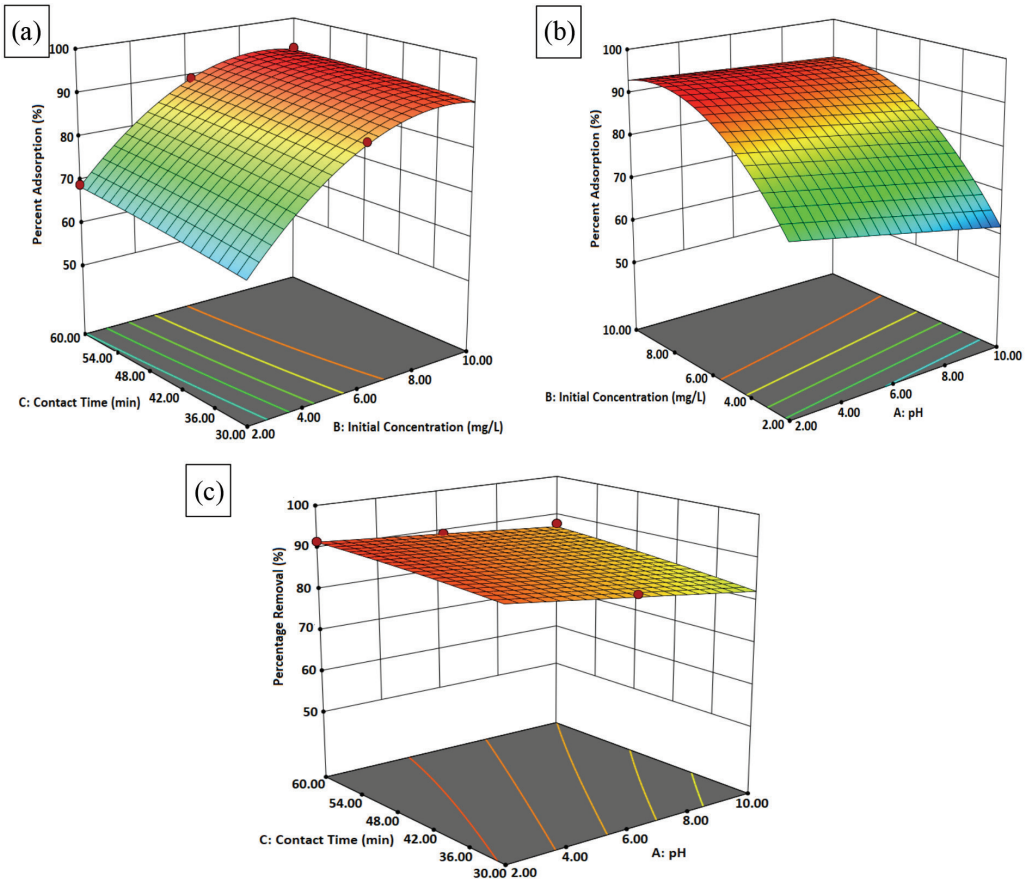

Figure 5: Graph of the combination effect of (a) contact time and initial concentrations, (b) initial concentration, and pH (c) contact time and pH

After 90 minutes of contact time and an initial concentration of 10 mg/L, a lower clearance was observed at pH 2 (89.78%). A solution's pH significantly impacts adsorption as it influences the adsorbent's surface charge and makes competing ions like H^+ and OH^- available. A positively charged SEAC surface is produced by the presence of H^+ ions at lower pH values (< pH 6) (Cheenmatchaya & Kungwankunakorn, 2013). Since MB is a cationic dye that needs a negatively charged adsorbent surface, this prevents it from adhering (Han *et al.*, 2020). The surface adsorbent adopts a negative surface at high pH, enhancing positive dyes' uptake via electrostatic attractions (Pathania *et al.*, 2017).

Conclusions

Sago effluent-derived activated carbon (SE-AC) has a better removal efficiency than SEB and has been effectively used as an adsorbent for MB in an aqueous solution. Based on the RSM parameters, the greatest removal effectiveness was 92.69% at pH 6, initial concentration (10 mg/L), and contact time (60 minutes). The adsorption with SEB exhibits a heterogeneous adsorption layer and is best fitted to the Freundlich isotherm while SEAC is best fitted to the Langmuir Isotherm. SEAC can be an effective adsorbent to mitigate environmental issues associated with sago industries. Its high adsorption capacity for contaminants such as

MB suggests it could significantly reduce the pollution load from sago processing effluents, thereby contributing to cleaner water bodies and a healthier ecosystem.

Acknowledgements

Thanks to Universiti Malaysia Sarawak and the funding provided by Tun Openg Sago Research Chair.

Conflict of Interest Statement

The authors declare that they have no conflict of interest.

References

Akila, E., Pugalendhi, S., Subramanian, P., Duraisamy, M. P., & Surendrakumar, A. (2019). Production and characterisation of activated carbon from date stones by single step steam activation. *Environment and Ecology*, *37*(October 2018), 194-197. https://www.cabdirect.org/cabdirect/abstract/20193125725

Aljeboree, A. M., Hussein, F. H., & Alkaim, A. F. (2019). Removal of textile dye (methylene blue MB) from aqueous solution by activated carbon as a model (corn-cob source waste of plant): As a model of environmental enhancement. *Plant Archives*, *19*, 906-909.

Amode, J. O., Santos, J. H., Md. Alam, Z., Mirza, A. H., & Mei, C. C. (2016). Adsorption of methylene blue from aqueous solution using untreated and treated (Metroxylon spp.) waste adsorbent: Equilibrium and kinetics studies. *International Journal of Industrial Chemistry*, *7*(3), 333-345. https://doi.org/10.1007/s40090-016-0085-9

Ao, W., Fu, J., Mao, X., Kang, Q., Ran, C., Liu, Y., Zhang, H., Gao, Z., Li, J., & Liu, Q. (2018). Microwave assisted preparation of activated carbon from biomass: A review. *Renewable and Sustainable Energy Reviews*, *92*(July 2017), 958-979. https://doi.org/10.1016/j.rser.2018.04.051

Araujo, L. K. F., Albuquerque, A. A., Ramos, W. C. O., Santos, A. T., Carvalho, S. H. V., Soletti, J, I., & Bispo, M. D. (2021). Elaeis guineensis-activatedcarbon for methylene blue removal: Adsorption capacity and optimisation using CCD-RSM. *Environment*, *Development and Sustainability*, *23*, 11732-11750. https://doi.org/10.1007/s10668-020-01137-7

Baalamurugan, J., Ganesh Kumar, V., Naveen Prasad, B. S., & Govindaraju, K. (2020). Removal of cationic textile dye methylene blue (mb) using steel removal of cationic textile dye methylene blue (MB) using steel slag composite. *Rasayan Journal Chemistry*, *13*(2), 1014-1021. https://doi.org/10.31788/RJC.2020.1325715

Buhani, Hariyanti, F., Suharso, Rinawati & Sumadi. (2019). Magnetised algae-silica hybrid from Porphyridium sp. biomass with Fe3O4 particle and its application as adsorbent for the removal of methylene blue from aqueous solution. *Desalination and Water Treatment*, *142*, 331-340. https://doi.org/10.5004/dwt.2019.23533

Chaduka, M., Guyo, U., Zinyama, N. P., & Matsinha, L. C. (2019). Modeling and optimisation of lead (ii) adsorption by a novel peanut hull-g-methyl methacrylate biopolymer using response surface methodology (RSM). *Analytical Letters*, *0*(0), 1-18. https://doi.org/10.1080/00032719.2019.1702993

Cheenmatchaya, A., & Kungwankunakorn, S. (2013). Preparation of activated carbon derived from rice husk by simple carbonisation and chemical activation for using as gasoline adsorbent. *International Journal of Environmental Science and Development*, *5*(2), 171-175. https://doi.org/10.7763/ijesd.2014.v5.472

Dahlan, N. A., Lee, L., & Pushmalar, J. (2019). Adsorption of methylene blue onto carboxymethyl sago pulp - immobilised sago waste hydrogel beads. *International Journal of Environmental Science and*

Technology, *16*, 2047-2058. https://doi.org/10.1007/s13762-018-1789-5

Devanna, N., Begum, B. A., & Chari, M. (2019). Low-cost adsorbents procedure by means of heavy metal elimination from wastewater. Preprints, 2019020013. https://doi.org/10.20944/preprints20190.0013.v1

Doke, K. M., & Khan, E. M. (2017). Equilibrium, kinetic and diffusion mechanism of Cr(VI) adsorption onto activated carbon derived from wood apple shell. *Arabian Journal of Chemistry*, *10*, S252-S260. https://doi.org/10.1016/j.arabjc.2012.07.031

dos Santos, K. J. L., de Souza dos Santos, G. E., de Sá, Í. M. G. L., de Carvalho, S. H. V., Soletti, J. I., Meili, L., de Silva Duarte, J. L., Bispo, M. D., & Dotto, G. L. (2019). Syagrus oleracea–activated carbon prepared by vacuum pyrolysis for methylene blue adsorption. *Environmental Science and Pollution Research*, *26*(16), 16470-16481. https://doi.org/10.1007/s11356-019-05083-4

Ebrahimi, P., & Kumar, A. (2021). Diatomite chemical activation for effective adsorption of methylene blue dye from model textile wastewater. *International Journal of Environmental Science and Development*, *12*(1). https://doi.org/10.18178/ijesd.2021.12.1.1313

Fazal, T., Faisal, A., Mushtaq, A., Hafeez, A., Javed, F., Din, A. A., & Rashid, N. (2019). Macroalgae and coal-based biochar as a sustainable bioresource reuse for treatment of textile wastewater. *Biomass Conversion and Biorefinery*, *5*(11), 1491-1506. https://doi.org/10.1007/s13399-019-00555-6

Gholamiyan, S., Hamzehloo, M., & Farrokhnia, A. (2020). RSM optimised adsorptive removal of erythromycin using magnetic activated carbon: Adsorption isotherm, kinetic modeling and thermodynamic studies. *Sustainable Chemistry and Pharmacy*, *17*(May), 100309. https://doi.org/10.1016/j.scp.2020.100309

González-García, P. (2018). Activated carbon from lignocellulosics precursors: A review of the synthesis methods, characterisation techniques and applications. *Renewable and Sustainable Energy Reviews*, *82*(August 2017), 1393-1414. https://doi.org/10.1016/j.rser.2017.04.117

Guo, F., Li, X., Jiang, X., Zhao, X., Guo, C., & Rao, Z. (2018). Characteristics and toxic dye adsorption of magnetic activated carbon prepared from biomass waste by modified one-step synthesis. *Colloids and Surfaces A: Physicochemical and Engineering Aspects*. https://doi.org/10.1016/j.colsurfa.2018.06.061

Hammado, N., & Utomo, S. (2018). Physicochemical characteristic of sago dregs and sago wastewater in luwu regency. *ICENIS*, *73*(7), 4-6. https://doi.org/10.1051/e3sconf/20187307007

Han, Q., Wang, J., Goodman, B. A., Xie, J., & Liu, Z. (2020). High adsorption of methylene blue by activated carbon prepared from phosphoric acid treated eucalyptus residue. *Powder Technology*, *366*, 239-248. https://doi.org/10.1016/j.powtec.2020.02.013

Hedge, G., Manaf, A. A. A., Kumar, A., Ali, G. A. M., Chong, K. F., Ngaini, Z., & Sharma, K. (2015). Biowaste sago bark based catalyst free carbon nanospheres: Waste to wealth approach. *ACS Sustainable Chemistry & Engineering*, 1-23.

Hu, X., & Gholizadeh, M. (2019). Biomass pyrolysis: A review of the process development and challenges from initial researches up to the commercialisation stage. *Journal of Energy Chemistry*, *39*, 109-143. https://doi.org/10.1016/j.jechem.2019.01.024

Husin, H., Ibrahim, M. F., Kamal Bahrin, E., & Abd-Aziz, S. (2019). Simultaneous saccharification and fermentation of sago dregs into biobutanol by Clostridium acetobutylicum ATCC 824. *Energy Science and Engineering*, *7*(1), 66-75. https://doi.org/10.1002/ese3.226

Islam, M. A., Ahmed, M. J., Khanday, W. A., Asif, M., & Hameed, B. H. (2017). Mesoporous activated carbon prepared from NaOH activation of rattan (Lacosperma secundiflorum) hydrochar for methylene blue removal. *Ecotoxicology and Environmental Safety*, *138*(August 2016), 279-285. https://doi.org/10.1016/j.ecoenv.2017.01.010

Janković, B., Manić, M., Dodevski, V., Radović, I., Pijović, M., Katnić, D., & Tasić, G. (2019). Physico-chemical characterisation of carbonised apricot kernel shell as precursor for activated carbon preparation in clean technology utilisation. *Journal of Cleaner Production*, *236*. https://doi.org/10.1016/j.jclepro.2019.117614

Jawad, A. H., Mohammaed, S. A., Mastuli, M. S., & Abdullah, M. F. (2018). Carbonisation of corn (Zea mays) cob agricultural residue by one-step activation with sulfuric acid for methylene blue adsorption. *Desalination and Water Treatment*, *118*(2018), 342-351. https://doi.org/10.5004/dwt.2018.22680

Jawad, A. H., Rashid, R. A., Ishak, M. A. M., & Wilson, L. D. (2016). Adsorption of methylene blue onto activated carbon developed from biomass waste by H2SO4 activation: Kinetic, equilibrium and thermodynamic studies. *Desalination and Water Treatment*, *57*(52), 25194-25206. https://doi.org/10.1080/19443994.2016.1144534

Kausar, R. A., Buhani & Suharso. (2020). Methylene blue adsorption isotherm on spirulina sp. microalgae biomass coated by silica-magnetite. *IOP Conference Series: Materials Science and Engineering*, *857*, 012019. https://doi.org/10.1088/1757-899X/857/1/012019

Khanday, W. A., Marrakchi, F., Asif, M., & Hameed, B. H. (2017). Mesoporous zeolite–activated carbon composite from oil palm ash as an effective adsorbent for methylene blue. *Journal of the Taiwan Institute of Chemical Engineers*, *70*, 32-41. https://doi.org/10.1016/j.jtice.2016.10.029

Kumar, J., Kaur, M., & Adiraju, B. (2018). Synthesis of activated carbon from agricultural waste using a simple method: Characterisation, parametric and isotherms study. *Materials Today: Proceedings*, *5*(2), 3334-3345. https://doi.org/10.1016/j.matpr.2017.11.576

Kumar, S., Pattnaik, D., Bhuyan, S. K., & Mishra, S. C. (2018). Influence of temperature on pyrolysis of biomass. *IOP Conference Series: Materials Science and Engineering*, *338*(1). https://doi.org/10.1088/1757-899X/338/1/012061

Kumar, V., Saharan, P., Sharma, A. K., Umar, A., Kaushal, I., & Mittal, A. (2020). Silver doped manganese oxide-carbon nanotube nanocomposite for enhanced dye-sequestration: Isotherm studies and RSM modelling approach. *Ceramics International*, *46*(8), 10309-10319. https://doi.org/10.1016/j.ceramint.2020.01.025

Lam, S. S., Liew, R. K., Wong, Y. M., Yek, P. N. Y., Ma, N. L., Lee, C. L., & Chase, H. A. (2017). Microwave-assisted pyrolysis with chemical activation, an innovative method to convert orange peel into activated carbon with improved properties as dye adsorbent. *Journal of Cleaner Production*, *162*, 1376-1387. https://doi.org/10.1016/j.jclepro.2017.06.131

Li, X., Han, D., Xie, J., Wang, Z., Gong, Z., & Li, B. (2018). Hierarchical porous activated biochar derived from marine macroalgae wastes (Enteromorpha prolifera): Facile synthesis and its application on methylene blue removal. *RSC Advances*, *51*, 29237-29247. https://doi.org/10.1039/c8ra04929g

Li, Z., Hanafy, H., Zhang, L., Sellaoui, L., Schadeck Netto, M., Oliveira, M. L. S., Seliem, M. K., Luiz Dotto, G., Bonilla-petriciolet, A., & Li, Q. (2020). Adsorption of congo red and methylene blue dyes on an ashitaba waste and a walnut shell-based

activated carbon from aqueous solutions: Experiments, characterisation and physical interpretations. *Chemical Engineering Journal*, *388*(January), 124263. https://doi.org/10.1016/j.cej.2020.124263

Makshut, N. A., Ngaini, Z., Wahi, R., Hussain, H., Mahmut, N. I., & Bahrin, N. Q. (2020). Nano-sized adsorbent from pyrolysed sago activated sludge for removal of pb(II) from aqueous solution. *Pertanika Journal of Science and Technology*, *28*(3), 893-916.

Mariathankam, A., Suruli, N., Setty, K., & Anand, B. (2020). Identification of hydrogen gas producing anaerobic bacteria isolated from sago industrial effluent. *Current Microbiology*, *77*(9), 2544-2553. https://doi.org/10.1007/s00284-020-02092-2

Marrakchi, F., Auta, M., Khanday, W. A., & Hameed, B. H. (2017). High-surface-are and nitrogen-rich mesoporous carbon material from fishery waste for effective adsorption of methylene blue. *Powder Technology*. https://doi.org/10.1016/j.powtec.2017.08.023

Mary, G. S., Niveditha, P. S. S., & Mary, G. S. (2016). Production, characterisation and evaluation of biochar from pod (Pisum sativum), leaf (Brassica oleracea) and peel (Citrus sinensis) wastes. *International Journal of Recycling of Organic Waste in Agriculture*, *5*(1), 43-53. https://doi.org/10.1007/s40093-016-0116-8

Miyah, Y., Lahrichi, A., Idrissi, M., Khalil, A., & Zerrouq, F. (2018). Adsorption of methylene blue dye from aqueous solutions onto walnut shells powder: Equilibrium and kinetic studies. *Surfaces and Interfaces*, *11*, 74-81. https://doi.org/10.1016/j.surfin.2018.03.006

Mookiah, V. P., Kasimani, R., Pandian, S., & Asokan, T. (2020). Study on the effects of initial pH, temperature and agitation speed on lipid production by yarrowia lipolytica and chlorella vulgaris using sago wastewater as a substrate. *Biocatalysis and Agrilcultural Biotechnology*, *40*, 692-703.

Nasrullah, A., Bhat, A. H., Naeem, A., Isa, M. H., & Danish, M. (2018). High surface area mesoporous activated carbon-alginate beads for efficient removal of methylene blue. *International Journal of Biological Macromolecules*, *107*, 1792-1799. https://doi.org/10.1016/j.ijbiomac.2017.10.045

Ngaini, Z. (2017). Facile sorbent from esterified cellulosic sago waste for engine oil removal in marine environment. *International Journal of Environmental Science and Technology*, *15*, 341-348. https://doi.org/10.1007/s13762-017-1389-9

Nibret, G., Ahmad, S., Govardhana, D., Ahmad, I., & Mohamed, S. (2019). Removal of methylene blue dye from textile wastewater using water hyacinth activated carbon as adsorbent: Synthesis, characterisation and kinetic studies. *Proceedings of International Conference on Sustainable Computing in Science*, *Technology and Management (SUSCOM)*. 1959-1969.

Pathania, D., Sharma, S., & Singh, P. (2017). Removal of methylene blue by adsorption onto activated carbon developed from Ficus carica bast. *Arabian Journal of Chemistry*, *10*, S1445-S1451. https://doi.org/10.1016/j.arabjc.2013.04.021

Patil, C. S., Kadam, A. N., Gunjal, D. B., & Naik, V. M. (2020). Separation and purification technology sugarcane molasses derived carbon sheet @ sea sand composite for direct removal of methylene blue from textile wastewater: Industrial wastewater remediation through sustainable, greener, and scalable methodology. *Separation and Purification Technology*, *247*(January), 116997. https://doi.org/10.1016/j.seppur.2020.116997

Pedicini, R., Maisano, S., Chiodo, V., Conte, G., Policicchio, A., & Agostino, R. G. (2020). Posidonia oceanica and wood chips activated carbon as interesting materials for hydrogen

storage. *International Journal of Hydrogen Energy*, *45*(27), 14038-14047. https://doi.org/10.1016/j.ijhydene.2020.03.130

Phang, S. M., Miah, M. S., Yeoh, B. G., & Hashim, M. A. (2000). Spirulina cultivation in digested sago starch factory wastewater. *Journal of Applied Phycology*, *12*, 395-400.

Priyanka, M., Kumar, D., Shankar, U., Yadav, A., & Yadav, K. (2018). Agricultural waste management for bioethanol production. In M. Priyanka (Ed.), *Handbook of research on microbial tools for environmental waste management* (pp. 1-33). IGI Global. https://doi.org/10.4018/978-1-5225-3540-9.ch001

Rafiq, M. K., Bachmann, R. T., Rafiq, M. T., Shang, Z., Joseph, S., & Long, R. (2016). Influence of pyrolysis temperature on physico-chemical properties of corn stover (zea mays l .) biochar and feasibility for carbon capture and energy balance. *PLOS ONE*, *11*(6), 1-17. https://doi.org/10.1371/journal.pone.0156894

Rahimian, R., & Zarinabadi, S. (2020). A review of studies on the removal of methylene blue dye from industrial wastewater using activated carbon adsorbents made from almond bark. *Journal of Environmental Health Science and Engineering*, *3*(3), 251-268.

Rajan, Y., Ngaini, Z., & Wahi, R. (2018). Novel adsorbent from sago-grafted silica for removal of methylene blue. *International Journal of Environmental Science and Technology*. https://doi.org/10.1007/s13762-018-2043-x

Rambli, J. Ghani, W. A. A. K., Salleh, M. A. M., & Khezri, R. (2019). Evaluation of biochar from sago (metroxylon spp.) as a potential solid fuel. *Journal of Engineering Science and Technology*, *14*(1), 1928-1940.

Rashid, J., Tehreem, F., Rehman, A., & Kumar, R. (2019). Synthesis using natural functionalisation of activated carbon from pumpkin peels for decolourisation of aqueous methylene blue. *Science of the Total Environment*, *671*, 369-376. https://doi.org/10.1016/j.scitotenv.2019.03.363

Reza, M., Dargahi, A., & Shabanloo, A. (2020). Electrochemical degradation of methylene blue dye using a graphite doped PbO2 anode: Optimisation of operational parameters, degradation pathway and improving the biodegradability of textile wastewater. *Arabian Journal of Chemistry*, *13*(8), 6847-6864. https://doi.org/10.1016/j.arabjc.2020.06.038

Sharma, A., Pareek, V., & Zhang, D. (2015). Biomass pyrolysis - A review of modelling, process parameters and catalytic studies. *Renewable and Sustainable Energy Reviews*, *50*, 1081-1096. https://doi.org/10.1016/j.rser.2015.04.193

Sheela, R., & Asha, B. (2020). A bio-kinetic study on liquid-to-biogas transfer in an up-flow anaerobic sludge fixed film reactor in the treatment of sago wastewater. *Desalination and Water Treatment*, *196*(September 2019), 433-438. https://doi.org/10.5004/dwt.2020.26083

Siruru, H., Syafii, W., Wistara, I. N. J., Pari, G., & Budiman, I. (2020). Properties of sago waste charcoal using hydrothermal and pyrolysis carbonisation. *Biomass Conversion and Biorefinery*, *12*, 5543-5554.

Somsesta, N., Sricharoenchaikul, V., & Aht-Ong, D. (2020). Adsorption removal of methylene blue onto activated carbon/cellulose biocomposite films: Equilibrium and kinetic studies. *Materials Chemistry and Physics*, *240*(September 2019), 122221. https://doi.org/10.1016/j.matchemphys.2019.122221

Su, Y., Liu, L., Xu, D., Du, H., Xie, Y., & Xiong, Y. (2020). Syngas production at low temperature via the combination of hydrothermal pretreatment and activated carbon catalyst along with value-added utilisation of tar and bio-char. *Energy Conversion and Management*, *205*(October 2019), 112382. https://doi.org/10.1016/j.enconman.2019.112382

Supriya, S., Sriram, G., Ngaini, Z., Mahaveer, C. K., Irene, K., & Padova, P. De. (2019). The role of temperature on physical-chemical properties of green synthesised porous carbon nanoparticles. *Waste and Biomass Valorisation*, (0123456789). https://doi.org/10.1007/s12649-019-00675-0

Teğin, İ., Öc, S., & Saka, C. (2024). Adsorption of copper (II) from aqueous solutions using adsorbent obtained with sodium hydroxide activation of biochar prepared by microwave pyrolysis. *Biomass Conversion and Biorefinery*, *15*, 12-14. https://doi.org/10.1007/s13399-024-05477-6

Üner, O., & Bayrak, Y. (2018). The effect of carbonisation temperature, carbonisation time and impregnation ratio on the properties of activated carbon produced from Arundo donax. *Microporous and Mesoporous Materials*, *268*, 225-234. https://doi.org/10.1016/j.micromeso.2018.04.037

Wahi, R., Aimi, S., Su, Y., Lam, S., Mona, S., Aziz, A., & Ngaini, Z. (2019). Esterification of microwave induced pyrolytic oil from sago bark waste. *Waste and Biomass Valorisation*, *11*, 3653-3663. https://doi.org/10.1007/s12649-019-00652-7

Wahi, R., Ngaini, Z., & Jok, V. U. (2009). Removal of mercury, lead and copper from aqueous solution by activated carbon of palm oil empty fruit bunch. *World Applied Sciences Journal*, *5*, 84-91.

Wahi, R., & Senghie, H. (2014). The use of microwave derived activated carbon for removal of heavy metal in aqueous solution. *Journal of Science and Technology*, *3*(1), 97-108.

Supplementary File

Table 1S: The physicochemical data of SE-B and SE-AC

Parameters	SEB	SEAC
BET (m^2/g)	8.04	76.86
Moisture content (%)	0.51 ± 0.02	0.00 ± 0.00
Volatile matter (%)	0.08 ± 0.02	0.00 ± 0.00
Ash content (%)	99.10 ± 0.03	99.90 ± 0.02
Fixed carbon (%)	0.22 ± 0.01	0.08 ± 0.01

Table 2S: Isotherm study on the adsorption of MB onto SE-AC

Isotherm	Parameters	SEB	SEAC
Langmuir	Q_{max} (mg/g)	-11.235	0.9012
	b (L/mg)	-0.139	13.940
	R^2	0.7438	0.9225
	R_L	1.385	0.034
Freundlich	n	-0.762	1.510
	1/n	-1.3129	0.7191
	K_f	0.5516	0.814
	R^2	0.9915	0.8527

Table 3S: Experimental factors and response for the adsorption of MB

Standard Run Number	Parameters			Response
	pH	Initial Concentration (mg/L)	Contact Time (min)	Adsorption (%)
1	2.00	2.00	30.00	69.30
2	10.00	2.00	30.00	58.15
3	2.00	10.00	30.00	92.17
4	10.00	10.00	30.00	88.11
5	2.00	2.00	90.00	72.35
6	10.00	2.00	90.00	67.15
7	2.00	10.00	90.00	89.78
8	10.00	10.00	90.00	91.45
9	6.00	6.00	60.00	88.73
10	6.00	6.00	60.00	89.25
11	6.00	6.00	60.00	88.95
12	6.00	6.00	60.00	88.95
13	2.00	6.00	60.00	91.51
14	10.00	6.00	60.00	87.70
15	6.00	2.00	60.00	69.05
16	6.00	10.00	60.00	92.69
17	6.00	6.00	30.00	86.67
18	6.00	6.00	90.00	89.57
19	6.00	6.00	60.00	88.73
20	6.00	6.00	60.00	88.95